European Review for Medical and Pharmacological Sciences 2015; 19: 2091-2104

Hsa-miR-206 represses the proliferation and invasion of breast cancer cells by targeting Cx43

Y. FU[1], Z.-M. SHAO[2], Q.-Z. HE[3], B.-Q. JIANG[1], Y. WU[1], Z.-G. ZHUANG[1]

[1]Department of Breast Surgery, Shanghai First Maternity and Infant Hospital, Tongji University School of Medicine, Shanghai, China
[2]Department of Breast Surgery, Fudan University Shanghai Cancer Center, Shanghai, China
[3]Department of Pathology, Shanghai First Maternity and Infant Hospital, Tongji University School of Medicine, Shanghai, China

Abstract. – OBJECTIVE: Hsa-miR-206, a microRNA, was found to be able to switch subtypes by targeting ER-α in breast cancer. However, there are few studies addressing the role of miR-206 in triple-negative breast cancer (TNBC). The purpose of this study was to evaluate the metastatic-regulatory ability of miR-206 in TNBC.

MATERIALS AND METHODS: We treated two TNBC lines (MDA-MB-231 and MDA-MB-436) with miR-206 mimics, inhibitors and paired controls and examined the *in vitro* and *in vivo* functions of miR-206 via the degradation of Connexin43 (Cx43). A luciferase reporter assay was used to identify the binding site of GJA1 (gap junctional intercellular communication) (Cx43) and miR-206. Furthermore, quantitative RT-PCR was used to evaluate miR-206 expression in 77 breast cancer samples to determine the association with lymph node status and Cx43 expression.

RESULTS: Up-regulation of miR-206 in TNBC contributed to a decreasing metastatic potential, as demonstrated by a reduction of cell viability and proliferation, decreased cell migration and invasion, lower expression levels of matrix metalloproteinase (MMP)-2, MMP-9 and a higher expression level of breast cancer metastatic suppressor (BRMS)-1. *In vitro* dual luciferase assays showed GJA1 (Cx43) is a target of miR-206. Quantitative RT-PCR was conducted to evaluate miR-206 expression in 77 breast cancer samples to determine the associations between miR-206 levels and both lymph node status and Cx43 expression. Restoring Cx43 expression positively regulated cell adhesion and GJA1, which may facilitate metastasis. MiR-206 significantly attenuated the proliferation and metastatic potential of cancer cells but did not inhibit tumor onset in a mouse xenograft model because of the dual function of Cx43.

CONCLUSIONS: Our results suggest hsa-miR-206 may repress the tumor proliferation and invasion in breast cancer by targeting Cx43.

Key Words:
Triple-negative breast cancer, Hsa-miR-206, Cx43, Metastasis, GJIC.

Introduction

Breast cancer has become the leading cause of malignant tumors in women. Although the 5 year survival rate for breast cancer has improved, there is still no targeted therapy available for triple-negative breast cancer (TNBC), defined histologically as invasive carcinoma of the breast that lacks staining for the estrogen receptor, progesterone receptor and human epidermal growth factor receptor-2. This type of breast cancer exhibits higher probabilities of recurrence and metastasis[1].

A class of small non-coding cellular RNAs termed microRNAs (miRNAs), which are approximately 22 nucleotides long, can repress their target genes by interfering with post-transcription pathways through cleaving mRNA molecules or inhibiting their translation[2]. In recent years, some miRNAs have been reported to be involved in cancer, playing important roles in many solid cancers, including breast cancer, pancreatic cancer, ovarian cancer and lung cancer[3,4]. There is substantial evidence indicating that some miRNAs can function as either oncogenes or tumor suppressors. For instance, miR-10b and miR-125b act as oncogenes, whereas miR-126 and miR-335 act as suppressors in breast cancer[5-8].

Hsa-miR-206 (miR-206) was the first microRNA found in breast cancer, and it plays an important role in cell apoptosis. This microRNA is regarded as a suppressor in many other cancers[9-12]. In breast cancer studies, a miR-206-binding site has been found within the 3'-untranslated region of ER-α, and this microRNA is present at higher

Corresponding Author: Zhigang Zhuang, Ph.D; e-mail: zhuang_zg@163.com

levels in MDA-MB-231 cells (ER-α negative) than in MCF-7 cells (ER-α positive)[13,14]. However, there are few studies addressing the role of miR-206 in TNBC. Thus, the aim of the present study was to evaluate the effect of miR-206 on the metastasis of TNBC.

Materials and Methods

Cell culture and Transfections

Human breast cancer cells were obtained from the Shanghai Fudan Breast Cancer Institute and were grown according to the culture conditions recommended by the ATCC. The MDA-MB-231 and MDA-MB-436 cells were transfected in 6-, 24- or 96- well plates with a hsa-miR-206 mimic (206m), inhibitor (206i) and paired negative controls (N.C. and I.N.C.) or with Cx43-siRNA, its paired N.C. (GenePharma, Shanghai, China, Table I) and the Cx43 plasmid, which was provided by the Department of Pathology and Cell Regulation of Kyoto Prefectural University of Medicine[15]. Transfection was performed with Lipofectamine™ 2000 (Invitrogen, Carlsbad, CA, USA), and then cells were cultured for 48 hours in a humidified 95% air/5% CO_2 atmosphere. Each group was divided into six types: wild-type, 206m-type, 206i-type and their paired negative controls (N.C. and I.N.C.).

Cell Viability Assay

Cells (2,000 cells/well) were plated in 96-well plates and prepared for transfection with 206m, 206i and their negative controls. After 48 hours, cell growth was evaluated via the Wst-8 assay using the Cell Counting Kit-8 (Dojindo, Kumamoto, Japan). The optical density (OD) at a wavelength of 450 nm was measured.

Quantitative Real-time PCR Analysis of miR-206

Quantitative analysis of miR-206 expression was performed using the Hairpin-it miRNAs qPCR Quantitation Kit (GenePharma, Shanghai, China) according to the manufacturer's instructions. The hsa-miR-206 and U6 snRNA primers employed for amplification are listed in Table II. U6 snRNA was used for normalization. The relative expression level of hsa-miR-206 was calculated as $2^{-\Delta\Delta Ct}$, where $^{\Delta}Ct$ = Ct (miR-206)-Ct (U6 snRNA).

Quantitative Real-time PCR Analysis of mRNAs and Immunoblotting

The levels of mRNA and protein expression of matrix metalloproteinase (MMP)-2, MMP-9, breast cancer metastatic suppressor (BRMS)-1, Connexin43 (Cx43) were determined by qPCR and immunoblotting. Glyceraldheyde 3-phosphate dehydrogenase (GAPDH) was employed for normalization. The primers used for amplification in qPCR are listed in Table II. The relative expression levels of mRNAs were calculated as $2^{-\Delta Ct}$. In immunoblotting, specific antibodies against MMP-2 (1:200, Abcam, Cambridge, MA, USA), MMP-9 (1:500, Abcam, Cambridge, MA, USA), BRMS-1 (1:1,000, Abcam), Cx43 (1:8,000, Abcam) and GAPDH (1:2,000, Aogma, Shanghai, China) were used according to standard protocols, and the resultant signals were detected using Image Lab 4.0 and Bio-Rad (Hercules, CA, USA) gel imaging system.

Cell Adhesion Assay

A 96-well plate was coated with 2 μg of 0.04 μg/μl Matrigel (BD Biosciences, Franklin LaKes, NJ, USA), after which 20 μl of medium containing 3% BSA (bovine serum albumin) was

Table I. Sequences of transfection agents.

Agent	Sequences
miR-206 mimics	5'-UGGAAUGUAAGGAAGUGUGUGG-3' 5'-ACACACUUCCUUACAUUCCAUU-3'
microRNA N.C	5'-UUCU CCGAAC GUGUCACGUTT-3' 5'-ACGUGACACGUUCGGAGAATT-3'
miR-206 inhibitors	5'-CCACACACUUCCUUACAUUCCA-3'
microRNA I.N.C	5'-CAGUACUUUUGUGUAGUACAA-3'
Cx43 siRNA	5'-GGCCUUGAAUAUCAUUGAATT-3' 5'-UUCAAUGAUAUUCAAGGCCTT-3'
siRNA N.C	5'-UUCUCCGAACGUGUCACGUTT-3' 5'-ACGUGACACGUUCGGAGAATT-3'

Table II. Specific primers of genes.

Genes	Primers
Hsa-miR-206	Forward: 5'- CAGATCCGATTGGAATGTAAGG-3' Reverse: 5'- TATGCTTGTTCTCGTCTCTGTGTC-3'
U6-snRNA	Forward: 5'- ATTGGAACGATACAGAGAAGATT-3' Reverse: 5'- GGAACGCTTCACGAATTTG-3'
Cx43	Forward: 5'-GGTGGACTGTTTCCTCTCTCG -3' Reverse: 5'-GGAGCAGCCATTGAAATAAGC -3'
MMP-2	Forward: 5'-GATACCCCTTTGACGGTAAGGA-3' Reverse: 5'-CCTTCTCCCAAGGTCCATAGC-3'
MMP-9	Forward: 5'-TGGGCTACGTGACCTATGACAT-3' Reverse: 5'-GCCCAGCCCACCTCCACTCCTC-3'
BRMS-1	Forward: 5'-TGCTGTCTCCATCCCTGAGC-3' Reverse: 5'- GGATGTGGCTTTGACTTCGG-3'
GAPDH	Forward: 5'-GGGAGCCAAAAGGGTCATCATCTC-3' Reverse: 5'-GGAGCAGCCATTGAAATAAGC -3'

added to each well. The procedure was carried out according to the reference[16]. The optical density (OD) of the plate was measured at a wavelength of 570 nm. The adhesion rate = (OD value of the experimental group-OD value of the control group)/OD value of the control group×100%. The wild-type subset of each group was used for normalization.

Cell Migration and Invasion

Migration and invasion experiments were conducted using transwell inserts (BD Biosciences, San Jose, CA, USA) and procedure was carried out according to reference[17]. Each well was incubated at 37°C for 18 hours for migration and 24 hours for invasion. After the filters were subsequently fixed, stained, they were analyzed under a light microscope at a magnification of 200×. Four fields were counted for each sample, after which the filters were washed with dimethyl sulfoxide (DMSO), and the optical density (OD) of the eluents was measured at a wavelength of 570 nm, with the wild-type subset of each group being used for normalization.

Scrape-Loading Dye Transfer Assay

The presence of functional gap junctions was evaluated through a scrape-loading dye transfer assay. Cells (2×10^5 cells/well) were co-transfected with a 206m or 206i and the Cx43 plasmid, Cx43-siRNA or a paired negative control and then plated in 6-well plates. The procedure was carried out according to el-Fouly et al[18]. The distance traveled by the dye perpendicular to the scrape was determined under an inverted fluorescence microscope.

In vivo Analysis

Female athymic (nu/nu) BALB/c mice at 4-6 weeks of age were obtained from the Shanghai Institute of Material Medica, Chinese Academy of Sciences (Shanghai, China) and housed in laminar flow cabinets under specific pathogen-free conditions. All mouse experiments were conducted in accordance with the NIH Guide for the Care and Use of Laboratory Animals. The study protocol was approved by the Animal Research Center of Tongji University. The tumorigenicity and spontaneous proliferative ability of the cell lines were determined via the injection of 1×10^6 cells in 0.1 ml of culture medium into the mammary fat pad[19]. The animals were divided into three groups: MDA-MB-231/wild-type, MDA-MB-231/206m and MDA-MB-231/206i. Each group contained six mice. The animals were killed and autopsied 8 weeks after inoculation. The tumor volume was calculated using the formula V=S×S×L/2 (S: the short length in mm; L: the longest length in mm). All tissues were prepared for hematoxylin and eosin (H&E) staining and immunohistochemistry using an anti-Cx43 antibody (1:4,000, Abcam) or anti-Ki-67 antibody (1:200, Dako, Glostrup, Denmark). All tissues were observed under a microscope (100× and 200×). The expression levels of Cx43 and Ki67 were analyzed in 10 different tumor fields, and the presence of these two proteins was assessed based on a four-point scale: -: < 10%; +: 11%~25%; ++: 26%~49%; +++: ≥ 50%. MMP-2, MMP-9 and BRMS-1 were detected via qPCR and immunoblotting to determine the metastatic potential of the cells.

Luciferase Reporter Assay

To perform reporter assays, psiCHECK-2/hsa-Cx43-3'UTR, psiCHECK-2/hsa-Cx43-mut-3'UTR or the control psiCHECK-2/vector (GenePharma, Paramount, CA, USA) was co-transfected with a 206m or N.C. into MDA-MB-231/436 cells in 96-well plates using Lipofectamine™ 2000 (Invitrogen). The resultant firefly and Renilla luciferase activities were measured using a dual luciferase assay (Promega, Madison, WI, USA) 48 hours after co-transfection. The firefly luciferase values were normalized to Renilla luciferase values.

Human Breast Cancer Sample Collection

A total of 77 patients with histologically confirmed invasive ductal carcinoma treated at Shanghai First Maternity and Infant Hospital from October 2011 to July 2012 were enrolled in this study. Primary breast tumors, paired peritumor tissue (breast tissue within 3 cm of the tumor) and normal breast tissue (breast tissue more than 3 cm from the tumor) were collected from each patient. The protocol was approved by the Human Research Ethics Committees of the hospital, and all samples were used after obtaining informed consent. All of the patients were undergoing surgery, displayed no distant metastases and hadn't received any therapy. The breast cancers were divided into four subtypes according to the highlights of 12th St. Gallen International Expert Consensus[20]. The patients' characteristics are shown in Table III. All samples were preserved at –80°C.

Table III. Patient characteristics in 77 cases of breast cancer

Characteristics	Num.	Percentage (%)
Age (years)		
– Median	56	
– Range	27~77	
– <56	37	48.1
– ≥56	40	51.9
Primary tumor size		
– T1	16	20.78
– T2	52	68.83
– T3	9	10.39
– T4	0	0
Lymphnode metastasis		
N0	39	50.65
N1-N3	38	49.35
Histological grade		
I	6	7.79
II	31	40.3
III	40	51.91
Subtype		
Luminal A	16	31.17
Luminal B	52	44.16
Her-2 overexpression	9	5.19
TNBC	0	19.48

Statistical Analysis

The statistical analyses were performed using SPSS 17.0 (SPSS Inc., Chicago, IL, USA). All cell culture data are presented as the mean±standard deviation (SD) and were evaluated using Student's *t* test. For nonparametric comparisons, univariate analyses were performed using the Mann Whitney-U test for two independent variables and the Kruskal-Wallis test for multi-independent variables. p values < 0.05 were considered statistically significant. Each assay was performed in triplicate.

Results

Hsa-miR-206 is Highly Expressed in TNBC Lines

Among the examined breast cancer cell lines, MDA-MB-468, MDA-MB-453, MDA-MB-436, MDA-MB-231 and the derived lung and bone metastasis lines (2m4, bo) are regarded as TNBC lines[21,22], whereas MCF-7, T47D and ZR-75-30 are regarded as luminal (ER-positive) breast cancer lines. By determining the expression level of hsa-miR-206 in each breast cancer cell line, we found it was higher in the TNBC cell lines than in the luminal cell lines. Its expression in MCF-10A cells was used for normalization (Figure 1 $p = 0.0000000011$). For example, the level of hsa-miR-206 was 6.64-fold higher in the MDA-MB-231 line than in the MCF-7 line. Furthermore, there were no differences among the TNBC lines (MDA-MB-468, MDA-MB-453, MDA-MB-436 and MDA-MB-231) ($p = 0.387$). We chose two TNBC lines (MDA-MB-231 and MDA-MB-436) to explore the role of hsa-miR-206 in TNBC in the present study.

Up-regulation of hsa-miR-206 Reduces the Viability of Breast Cancer Cells

Following transfection, we employed qPCR of hsa-miR-206. Compared to the levels in all of the negative controls, the expression level of hsa-miR-206 in MDA-MB-231/436 cells differed significantly (Figure 2A). Transfection with 206m resulted in reduced cell viability compared to

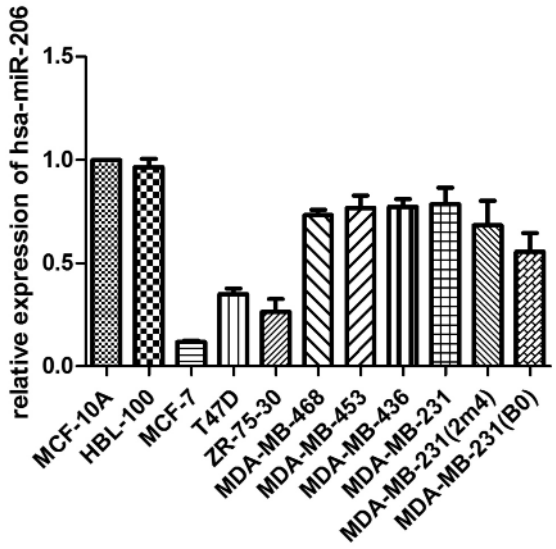

Figure 1. Hsa-miR-206 expression in breast cancer cell lines. Expression was detected via real-time PCR. The expression level in MCF-10A cells was used for normalization.

transfection with the N.C. (*p*: 0.037 *vs.* 0.011), and transfection with 206i resulted in enhanced cell viability compared with transfection with the I.N.C. (*p:* 0.022 *vs.* 0.042) (Figure 2B).

Up-regulation of hsa-miR-206 Reduces the Metastatic Ability of Breast Cancer Cells in vitro

On the one hand, we analyzed several relevant effector molecules, including MMP-2, MMP-9 and BRMS-1. QPCR revealed 206m-transfected cells expressed lower levels of MMP-2 ($p = 0.031$ *vs.* $p = 0.021$) and MMP-9 ($p = 0.020$ *vs.* $p = 0.007$) and a higher level of BRMS-1 ($p = 0.044$ *vs.* $p = 0.009$) compared to N.C.-transfected cells, whereas opposite results were found for 206i-transfected cells (MMP-2: $p = 0.031$ *vs.* $p = 0.006$; MMP-9: $p = 0.027$ *vs.* $p = 0.034$; BRMS-1: $p = 0.042$ *vs.* $p = 0.001$)

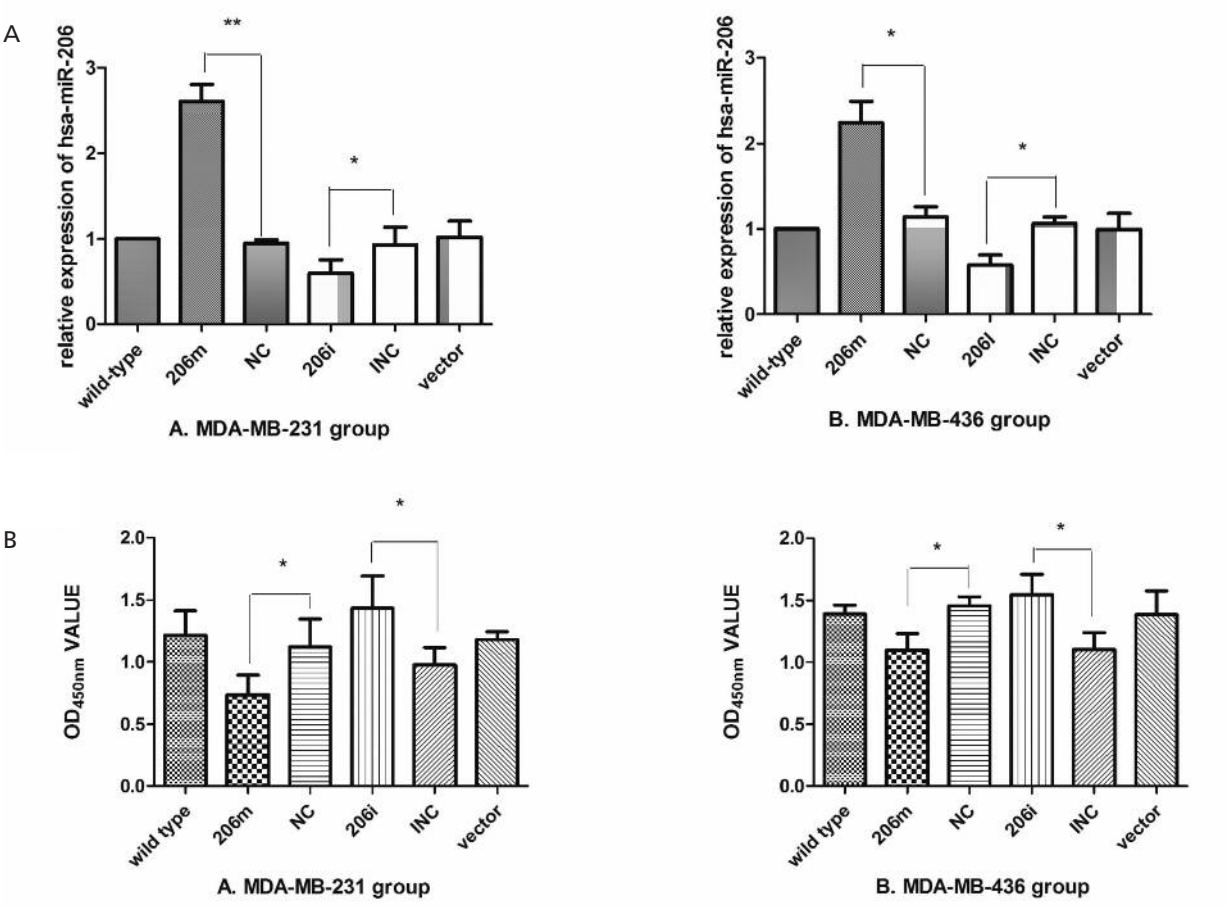

Figure 2. Up-regulation of hsa-miR-206 reduces the viability of breast cancer cells. (**A**) The relative expression levels of hsa-miR-206 following transfection determined via qPCR. The wild-type subset of each group was used for normalization. (**B**) Cell viability following transfection measured via CCK-8. *: $p < 0.05$; **: $p < 0.01$.

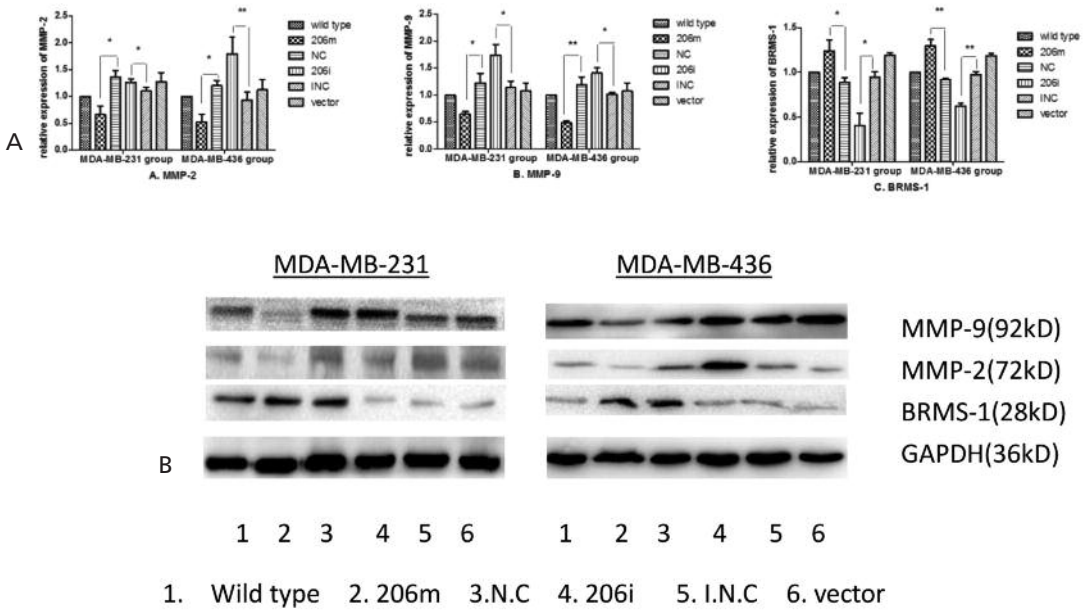

Figure 3. Up-regulation of has-miR-206 reduces the metastatic ability of breast cancer cells. (**A**) The relative expression levels of mRNAs detected via qPCR. The wild-type subset of each group was used for normalization. *: $p < 0.05$; **: $p < 0.01$. (**B**) Expression of metastasis-related molecules via immunoblotting. 1. Wild-type; 2. 206m; 3. N.C.; 4. 206i; 5. I.N.C.; 6. Vector.

compared to I.N.C.-transfected cells (Figure 3A). Similar results were obtained via immunoblotting (Figure 3B).

On the other hand, we performed migration and invasion experiments using a classic Transwell assay to detect the mobility. As shown in Figure 4, 206m transfection resulted in a significant decrease compared to N.C. transfection ($p_{migration}$: 0.003 *vs.* 0.001; $p_{invasion}$: 0.002 *vs.* 0.013), whereas opposite results were obtained for 206i-transfected cells compared to I.N.C.-transfected cells ($p_{migration}$: 0.001 *vs.* 0.005; $p_{invasion}$: 0.035 *vs.* 0.007).

Hsa-miR-206 Inhibits Tumor Proliferation and Invasion in vivo

To address whether miR-206 inhibits metastatic behavior *in vivo*, we implanted 206m/206i-transfected or wild-type MDA-MB-231 cells into the mammary fat pads of mice (Figure 5A). At 4 weeks post implantation, the xenograft tumors in all groups were of comparable size (Figure 5B), and the primary tumors formed by the 206m-transfected cells were statistically significantly bigger than those formed by wild-type cells eight weeks after orthotopic transplantation ($p = 0.028$). To determine

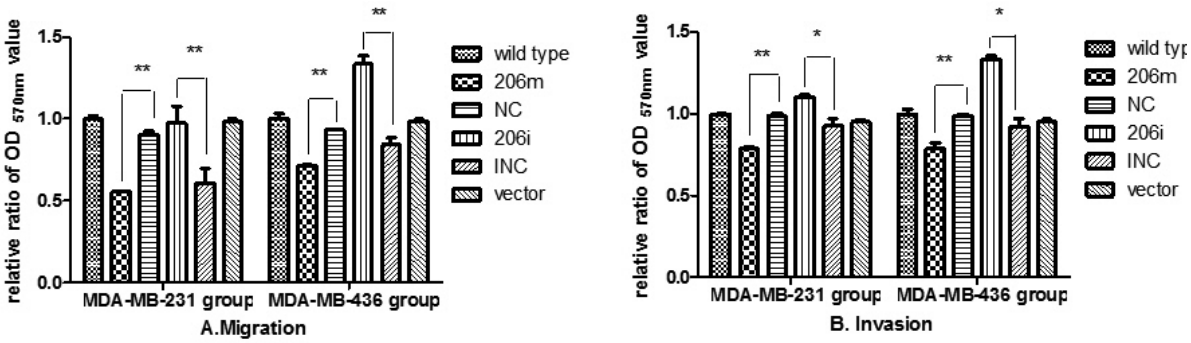

Figure 4. The migration and invasion of transfected breast cancer cells. The optical density $(OD)_{570\ nm}$ was measured, with the wild-type subset of each group being used for normalization. *: $p < 0.05$; **: $p < 0.01$.

whether miR-206 expression in primary tumors also affects the proliferation and invasive potential of cells, we analyzed the Ki-67 proliferation marker and Connexin43 (Cx43) via immunohistochemistry. We found although miR-206 overexpression induced tumor growth, it greatly reduced Cx43 expression and contributed to decreasing the number of Ki-67$^+$ cells and *vice versa* (Figure 5C). Furthermore, we assessed MMP-2, MMP-9 and BRMS-1 via qPCR and immunoblotting to determine the metastatic potential of the cells. We found the xenograft tumors formed by 206m-transfected cells exhibited a lower expression levels of MMP-2 (p = 0.006) and MMP-9 (p = 0.028) and a higher expression level of BRMS-1 (p = 0.031) compared to wild-type tumors. The results for the 206i-transfected tumors showed opposite trends, although only the MMP-9 expression level was significantly different (p = 0.013, Figure 5D). These results were consistent with the immunoblotting results (Figure 5E), indicating that up-regulation of miR-206 results in decreases in proliferation and metastatic potential, even though the tumors were larger.

Cx43 is a Target of hsa-miR-206 in Breast Cancer Cells

We used the TargetScan, PicTar and miRanda databases to identify potential hsa-miR-206 target genes, and we identified GJA1 (NM_000165, Cx43) as a target of hsa-miR-206. Through qPCR (Figure 6A), we found 206m transfection reduced Connexin43 expression (p = 0.009 *vs.* p = 0.031), whereas 206i-transfected cells displayed enhanced Connexin43 expression (p = 0.043 *vs.* p = 0.032). We obtained similar results for Cx43 via immunoblotting (Figure 6B).

To determine whether Cx43 is a direct target of hsa-miR-206, luciferase reporters containing the Cx43 3'-UTR or a Cx43 mut 3'-UTR were constructed and co-transfected with miRNA mimics or the negative control into MDA-MB-231/436 cells (Figure 6C). Compared to the control, the overexpression of hsa-miR-206 decreased the luciferase activity of the reporter construct containing the Cx43 3'-UTR by approximately 57.34% in MDA-MB-231 cells (p = 0.035) and by approximately 54.77% in MDA-MB-436 cells (p = 0.026), indicating that Cx43 is a direct target of hsa-miR-206.

Restoring Cx43 Expression Positively Regulates cell Adhesion and gap Junctional Intercellular Communication (GJIC)

After confirming Cx43 is downstream of hsa-miR-206, we co-transfected a Cx43 plasmid, Cx43-siRNA or a paired negative control with a 206m or 206i into MDA-MB-231 cells to determine whether Cx43 is involved in tumor metastasis. In adhesion assays (Figure 7A), we observed the Cx43-siRNA-transfected cells displayed a lower adhesion ability (p = 0.002), whereas the Cx43 plasmid-transfected cells exhibited a higher adhesion ability (p = 0.039). In the co-transfection experiments, we found regardless of the miR-206 expression level in cells, restoring Cx43 expression also resulted a statistically higher adhesion ability (p = 0.044 *vs.* p = 0.020). Furthermore, in cells overexpressing miR-206, knockdown of Cx43 expression via Cx43-siRNA transfection resulted in a decreased adhesion ability (p = 0.024). In scrape-loading dye transfer assays, GJIC was found to be decreased in the Cx43-siRNA-transfected cells and increased in the Cx43 plasmid-transfected cells, regardless of the level of miR-206 expression (Figure 7B).

Hsa-miR-206 and Cx43 Expression Are Correlated With the Subtypes and Lymph Node Statuses of Breast Cancer Patients

Firstly, we detected the hsa-miR-206 expression levels in primary breast tumors, paired peritumor tissues and normal breast tissues. The expression level in normal breast tissues was used for normalization. By qPCR, we found the expression of hsa-miR-206 was lower in paired peritumor tissues and lowest in breast tumors. Furthermore, the expression of hsa-miR-206 was significantly different among the subtypes of primary breast tumors (p = 0.003), whereas there were no differences detected among the paired peritumor tissues (p = 0.172). But no differences were observed between the two luminal subtypes (p = 0.690) or between the Her-2-overexpressing and TNBC subtypes (p = 0.637). However, the expression levels recorded in the Her-2-overexpressing subtype and the TNBC subtype were significantly higher than that in the luminal subtype ($p_{\text{luminal A-Her-2-overexpressing}}$: 0.034; $p_{\text{luminal B-Her-2-overexpressing}}$: 0.001; $p_{\text{luminal A-TNBC}}$: 0.027; $p_{\text{luminal B-TNBC}}$: 0.006). Thus, the expression of hsa-miR-206 was correlated

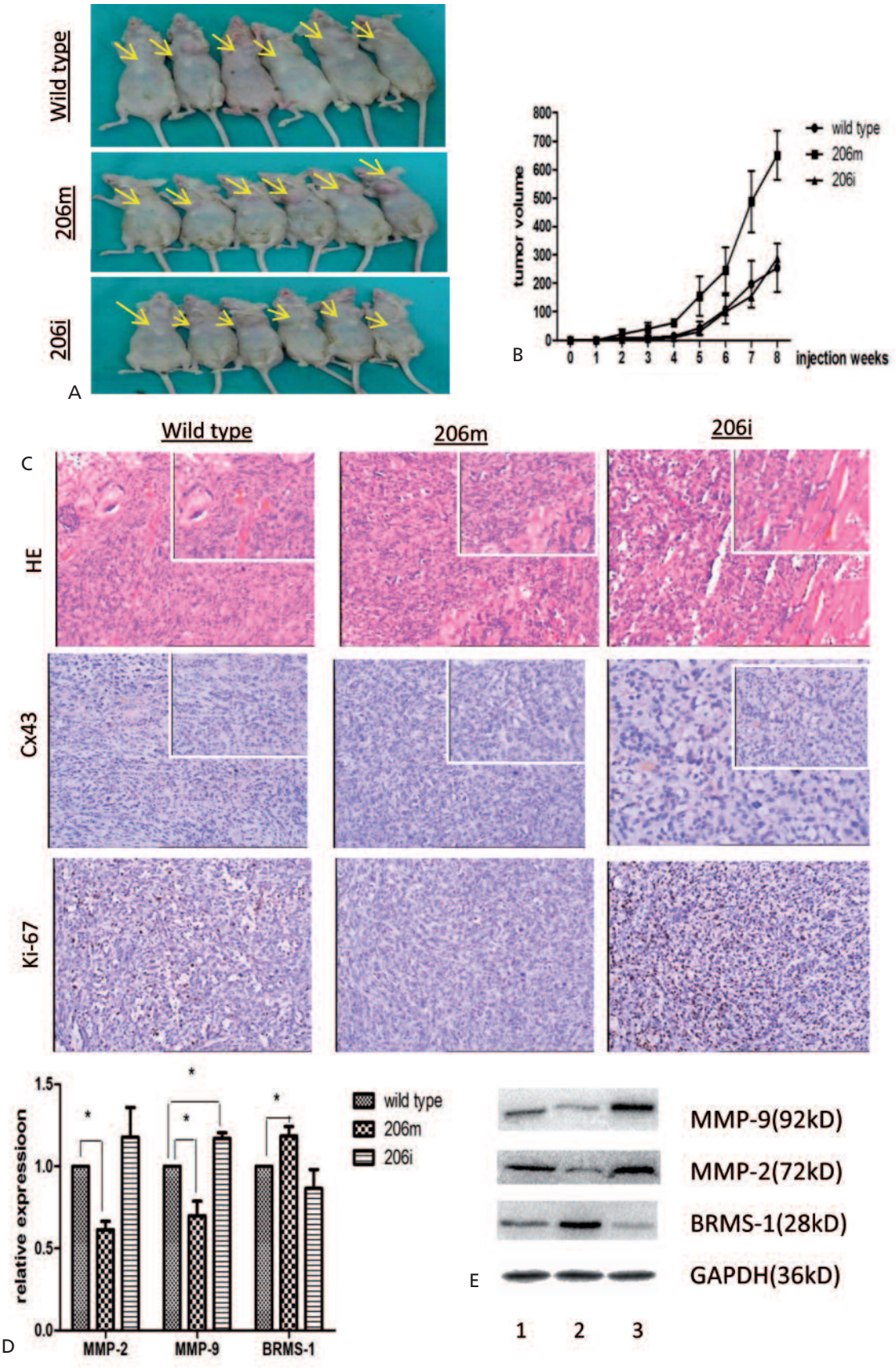
Wild type
206m
206i
A
tumor volume
800
700
600
500
400
300
200
100
0
0 1 2 3 4 5 6 7 8
injection weeks
wild type
206m
206i
B
Wild type
206m
206i
C
HE
Cx43
Ki-67
relative expressioon
1.5
1.0
0.5
0.0
MMP-2
MMP-9
BRMS-1
wild type
206m
206i
D
MMP-9(92kD)
MMP-2(72kD)
BRMS-1(28kD)
GAPDH(36kD)
E
1 2 3

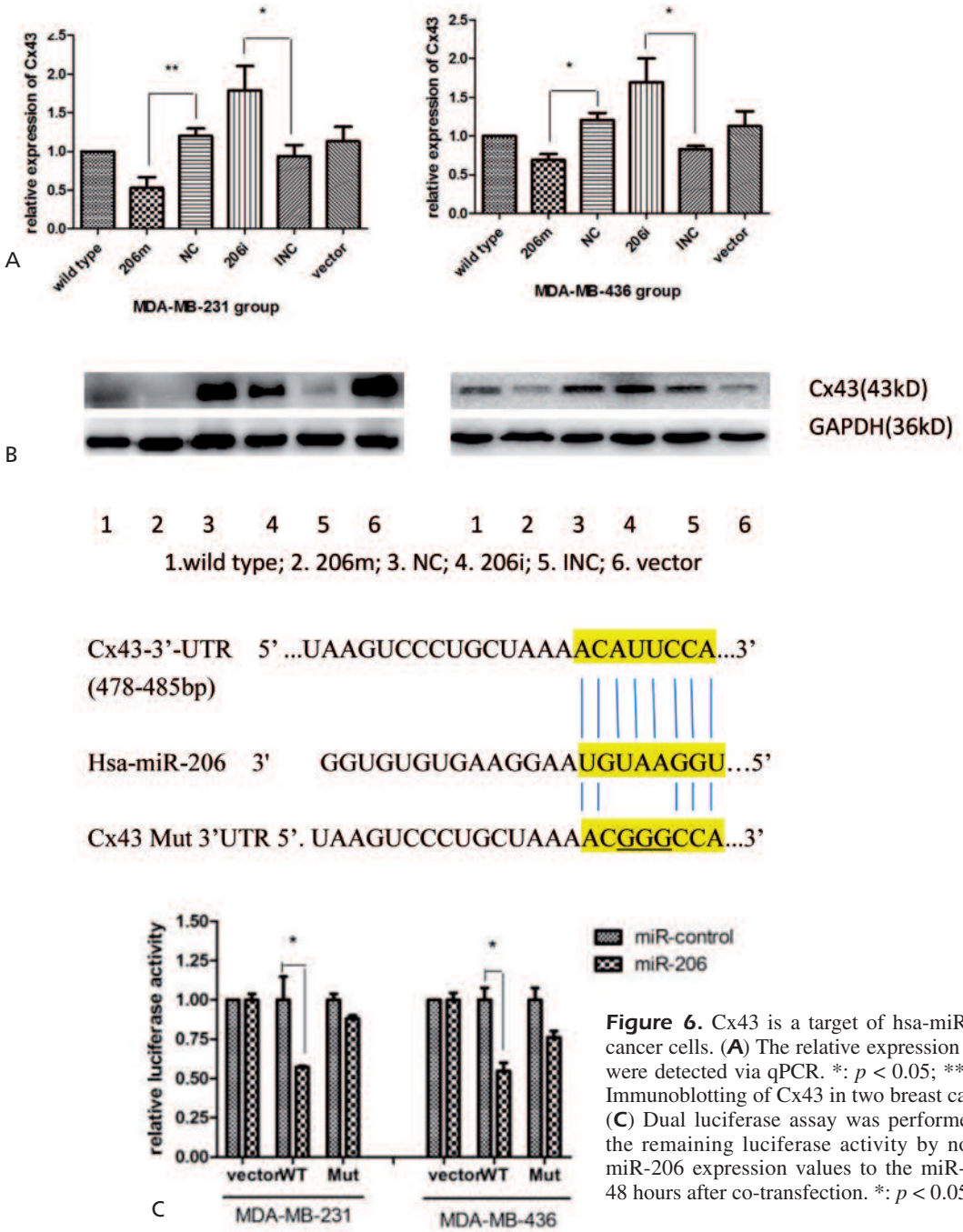

Figure 6. Cx43 is a target of hsa-miR-206 in breast cancer cells. (**A**) The relative expression levels of Cx43 were detected via qPCR. *: $p < 0.05$; **: $p < 0.01$. (**B**) Immunoblotting of Cx43 in two breast cancer cell lines. (**C**) Dual luciferase assay was performed to calculate the remaining luciferase activity by normalizing the miR-206 expression values to the miR-control values 48 hours after co-transfection. *: $p < 0.05$; **: $p < 0.01$.

Figure 5. Hsa-miR-206 inhibits tumor proliferation and invasion *in vivo*. (**A**) Mice and tumors formed by MDA-MB-231 cells transfected with a hsa-miR-206 mimic or inhibitor 8 weeks after orthotopic transplantation. (**B**) Growth curves for xenograft mammary tumors. (**C**) Hematoxylin and eosin (H&E)-, Cx43- and Ki-67-stained sections of xenograft mammary tumors. Magnification: ×100 (upper-right corner of each panel: ×200). (**D**) The relative expression levels of MMP-2, MMP-9 and BRMS-1 were detected via quantitative real-time PCR. *: $p < 0.05$; **: $p < 0.01$. (**E**) The expression levels of MMP-2, MMP-9 and BRMS-1 were detected via immunoblotting.

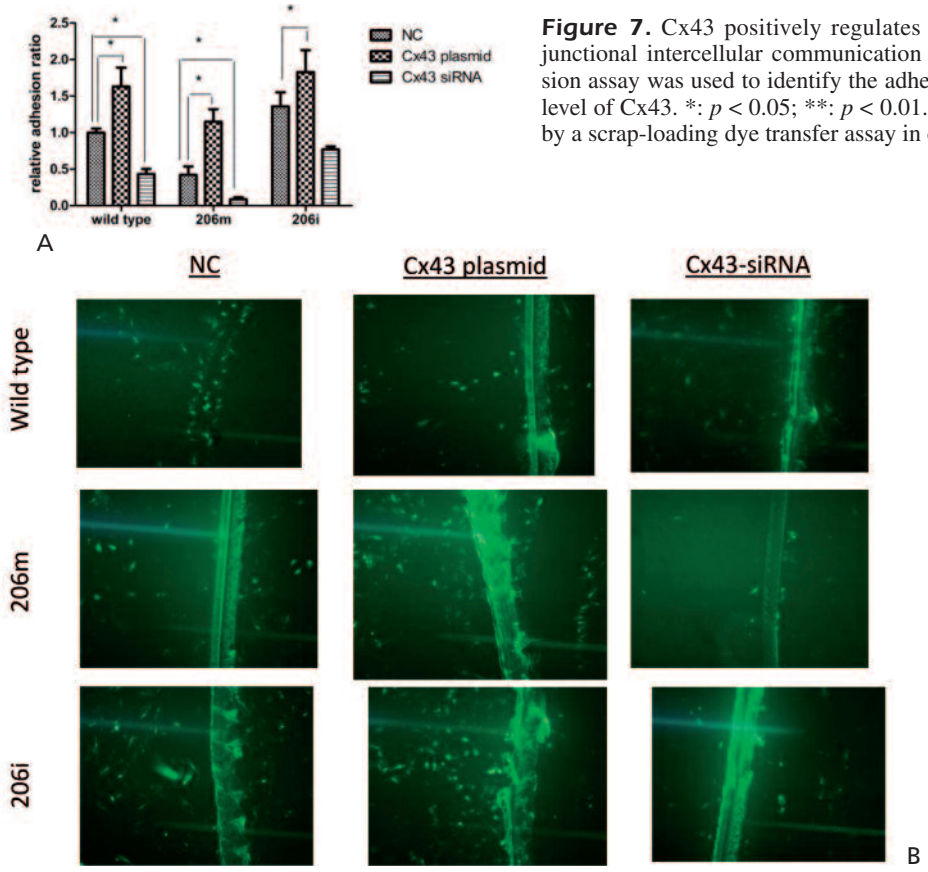

Figure 7. Cx43 positively regulates cell adhesion and gap junctional intercellular communication (GJIC). (**A**) The adhesion assay was used to identify the adhesion ability of different level of Cx43. *: $p < 0.05$; **: $p < 0.01$. (**B**) GJIC was detected by a scrap-loading dye transfer assay in different level of Cx43.

with ER status, being lower in ER-positive breast cancer than in ER-negative breast cancer.

When analyzing lymph node status, we found the expression of hsa-miR-206 was statistically higher in the lymph node-negative group than in the lymph node-positive group ($p = 0.036$, Figure 8A).

Secondly, as shown in Figure 8B, we sought to assess the expression of Cx43 in breast tumors. QPCR analysis revealed there was a statistically significant difference in Cx43 expression among subtypes ($p = 0.003$). In this analysis, the expression level in the luminal subtypes was used for normalization. Cx43 expression was lower in the Her-2-overexpressing subtype ($p = 0.002$) and TNBC subtype ($p = 0.002$) than in the luminal subtypes, but there was no difference between the Her-2-overexpressing and TNBC subtypes ($p = 0.749$). In addition, the Cx43 expression level was significantly different between patients with different lymph node statuses ($p = 0.00025$). The expression of Cx43 in the lymph node-negative group was used for normalization. Thirdly, similar results via immunoblotting was shown in Figure 8C.

Discussion

Metastasis is a complex, multi-step process involving adhesion, enzymatic degradation, movement and proliferation from microscopic foci into macroscopic secondary tumors. There are a growing number of studies addressing miRNAs, some of which classified as oncogenes or tumor-suppressor genes in different types of tumors. In the present study, we chose MDA-MB-231 and MDA-MB-436 cells as models to analyze cell proliferation, adhesion, migration and invasion in response to different levels of miR-206 because they are ER-α(-)/PgR(-), do not express Her-2 and are capable of metastasizing. Finally, we found up-regulation of hsa-miR-206 reduced cell viability and proliferation and inhibited cell migration and invasion in Transwell assays, while down-regulation of hsa-miR-206 had the opposite effect.

Many genes are involved in the cascade reaction, including metastasis promoter genes and suppressor genes. MMPs, a group of zinc-containing enzymes that are responsible for the degradation of extracellular matrix components,

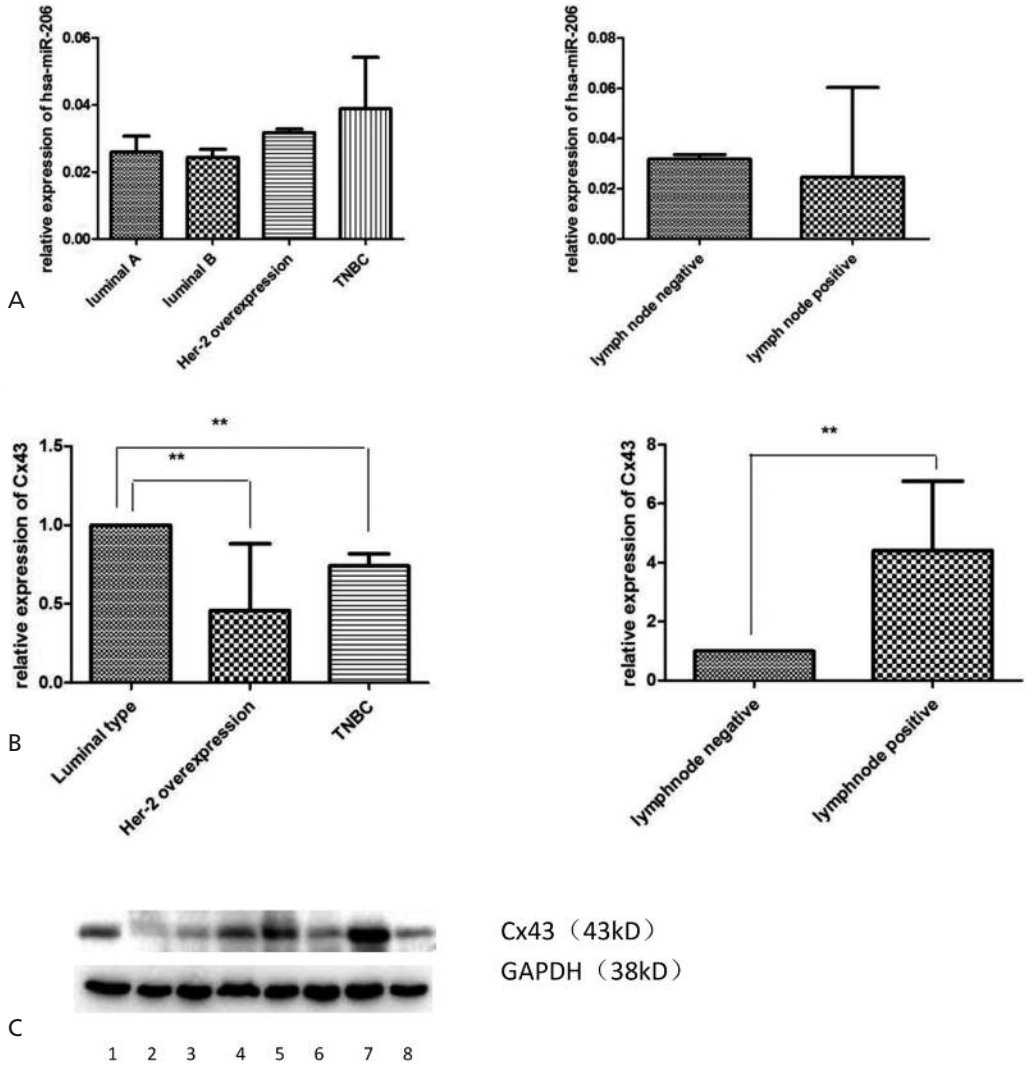

Figure 8. hsa-miR-206 and Cx43 expression levels are correlated with the subtype and lymph node status of breast cancer samples. (**A**) The expression of hsa-miR-206 was qPCR to analyze the correlation with ER status and lymph node status. *: $p < 0.05$; **: $p < 0.01$. (**B**) The expression of Cx43 was detected via qPCR to analyze the relationship with subtypes and lymph nodes status. *: $p < 0.05$; **: $p < 0.01$. (**C**) Immunoblotting of breast tumors. 1, 2, 3: lymph node negative; 4, 5, 6, 7, 8: lymph node positive; 1, 5, 7: luminal subtype; 2, 6: Her-2-overexpressing subtype; 3, 4, 8: TNBC subtype.

play pivotal roles in tumor growth, invasion and metastasis. BRMS-1, one kind of metastasis suppressors, exhibits low expression levels in melanoma, breast cancer and ovarian cancer, blocking the ability of cancer cells to metastasize but unblocking the formation of orthotopic tumors[22]. In the present study, we found up-regulation of hsa-miR-206 reduced the expression of MMP-2 and MMP-9 and increased the level of BRMS-1, indicating that hsa-miR-206 might decrease the metastatic potential.

It is well established that miRNAs function via the repression of target gene translation. Several targets of miR-206 have been identified thus far. In human mesenchymal stem cell-derived neuronal cells, researchers found miR-206 regulates the synthesis of the neurotransmitter substance P by targeting Tac1[23]. MET is directly targeted by miR-206 as a biomarker for early diagnosis of papillary thyroid carcinoma[24]. MiR-206 may function as a tumor suppressor by targeting notch3 in HeLa cells, resulting in activation of apoptosis and inhibition of tumor cell migration[25]. In a study addressing breast cancer, miRNA-206 was shown to target ER-α, the expression of which was strongly inhibited by

ERαagonists[13], contributed to switching from a luminal-A phenotype to a basal-like phenotype[27]. In the present study, we analyzed the expression of miR-206 in primary breast tumor samples and found it was higher in the Her-2-overexpressing and TNBC subtypes than in luminal subtypes at both the mRNA and protein levels. These results suggest the expression of this microRNA is correlated with ER-α status, similar to the findings of the studies mentioned above[13,27].

By utilizing multiple target prediction tools, combining bioinformatics and experimental approaches, we determined Cx43 expression is regulated by miR-206 in breast cancer cells through a target site in the 3'-UTR.

Cx43, a member of the connexin family of proteins, is abundant in breast tissues and helps regulate gap junctional intercellular communication (GJIC). GJIC is defined as a process in which small molecules (< 1,000 Da), such as ions and secondary messengers, can be transferred between adjoining cells through physical channels composed of connexons located in the plasma membrane. Connexins appear to regulate several genes involved in tumor onset, progression and metastasis[28]. GJIC is a complex process that is capable of inhibiting or promoting the migratory and invasive qualities of cancer cells because tumor cells can display homotypic (tumor cell-tumor cell) or heterotypic (tumor cell-host cell) interactions[29].

In view of their roles, connexins and GJIC are regarded as paradoxical in the process of tumorigenesis and metastasis. Restoration of GJIC through the expression of connexins in some models decreases tumorigenesis, but emerging evidence suggests gap junctions act as tumor suppressors in the initial stages of this process, whereas the re-expression of connexins in migrating tumor cells might facilitate invasion, intravasation, extravasation and metastasis in late-stage disease[30,31].

In the present study, we firstly analyzed the expression of miR-206 in different human breast cancer cells. We found microRNA-206 is highly expressed in TNBC cells compared to luminal breast cancer cells. This result is in accordance with the expression levels of miR-206 detected in clinical samples, which might arise from the regulation of ER by miR-206[13,14]. Our research was focused on the function of miR-206 in TNBC.

We, further, assessed the expression of hsa-miR-206 under different levels of Cx43, and a negative correlation was observed, exactly mimicking the relationship between Cx43 and hsa-miR-206 in clinical samples. Furthermore, we found at any level of miR-206, restoring Cx43 expression enhanced cell adhesion and GJIC via scrape-loading dye transfer assays. In cells overexpressing miR-206, the knockdown of Cx43 expression via transfection with Cx43 siRNA resulted in the lowest observed adhesion ability and strongly reduced GJIC. In our *in vivo* analysis, although higher expression of miR-206 was associated with larger xenografts, it attenuated the proliferation and metastatic potential of the tumors, which was consistent with the *in vitro* findings. This result might be due to the dual function of Cx43. During tumor onset, when Cx43 is down-regulated, gap junctions may not be assembled, thus, reducing or eliminating homotypic interactions. The exchange of small molecules decreases, which may activate abnormal signaling pathways that promote proliferation. However, as the disease advances and tumor cells enter the vasculature, the restoration of connexins results in gap junction opening, especially in heterotypic interactions, to facilitate invasion, intravasation, extravasation and metastasis.

TNBC is associated with high rates of proliferation and metastasis, early recurrence and poor survival rates, and the clinical treatments available for this type of cancer are limited. Therefore, targeting miRNAs and connexins could be considered a potential therapeutic strategy as part of a multi-gene treatment approach. Our data suggest enhanced expression of miR-206 in breast cancer cells represses the invasive and metastatic potential of the cells by targeting Cx43, which positively regulates GJIC and facilitates late-stage disease progression.

Conclusions

Although further work is required to fully understand the mechanism of GJIC, the *in vitro* and *in vivo* functions of miR-206 has been identified via degradation of Cx43. Our results showed up-regulation of miR-206 in TNBC contributed to a decreasing metastatic potential, and restoring Cx43 expression positively regulated cell adhesion and GJIC, which may facilitate metastasis. This finding may lead to the development of an effective treatment strategy for TNBC.

Acknowledgements

We thank Shanghai Fudan Breast Cancer Institute for providing cancer cell lines and Dr. Tetsuro Takamatsu of Department of Pathology and Cell Regulation of Kyoto Prefectural University of Medicine for kindly donating the Cx43 plasmid. This work was supported by the following grants: Shanghai Health Bureau (20114y155, 20124164), Science and Technology Commission of Shanghai Municipality (124119a4700).

Conflict of interest

The Authors declare that there are no conflicts of interest.

References

1) Dent R, Trudeau M, Pritchard KI, Hanna WM, Kahn HK, Sawka CA, Lickley LA, Rawlinson E, Sun P, Narod SA. Triple-negative breast cancer: clinical features and patterns of recurrence. Clin Cancer Res 2007; 13: 4429-4434.
2) Bartel DP. MicroRNAs: genomics, biogenesis, mechanism, and function. Cell 2004; 116: 281-297.
3) Budhu A, Ji J, Wang XW. The clinical potential of microRNAs. J Hematol Oncol 2010; 3: 37.
4) Yang J, Zeng Y. Identification of miRNA-mRNA crosstalk in pancreatic cancer by integrating transcriptome analysis. Eur Rev Med Pharmacol Sci, 2015; 19: 825-834.
5) Negrini M, Calin GA. Breast cancer metastasis: a microRNA story. Breast Cancer Res BCR 2008; 10: 203.
6) Ma L, Teruya-Feldstein J, Weinberg RA. Tumour invasion and metastasis initiated by microRNA-10b in breast cancer. Nature 2007; 449: 682-688.
7) Zhu S, Wu H, Wu F, Nie D, Sheng S, Mo YY. MicroRNA-21 targets tumor suppressor genes in invasion and metastasis. Cell Res 2008; 18: 350-359.
8) Lowery AJ, Miller N, McNeill RE, Kerin MJ. MicroRNAs as prognostic indicators and therapeutic targets: potential effect on breast cancer management. Clin Cancer Res 2008; 14: 360-365.
9) Hidaka H, Seki N, Yoshino H, Yamasaki T, Yamada Y, Nohata N, Fuse M, Nakagawa M, Enokida H. Tumor suppressive microRNA-1285 regulates novel molecular targets: aberrant expression and functional significance in renal cell carcinoma. Oncotarget 2012; 3: 44-57.
10) Vickers MM, Bar J, Gorn-Hondermann I, Yarom N, Daneshmand M, Hanson JE, Addison CL, Asmis TR, Jonker DJ, Maroun J, Lorimer IA, Goss GD, Dimitroulakos J. Stage-dependent differential expression of microRNAs in colorectal cancer: potential role as markers of metastatic disease. Clin Exp Metastasis 2012; 29: 123-132.
11) Zhang T, Liu M, Wang C, Lin C, Sun Y, Jin D. Down-regulation of MiR-206 promotes proliferation and invasion of laryngeal cancer by regulating VEGF expression. Anticancer Res 2011; 31: 3859-3863.
12) Chen X, Yan Q, Li S, Zhou L, Yang H, Yang Y, Liu X, Wan X. Expression of the tumor suppressor miR-206 is associated with cellular proliferative inhibition and impairs invasion in ERalpha-positive endometrioid adenocarcinoma. Cancer Lett 2012; 314: 41-53.
13) Adams BD, Furneaux H, White BA. The micro-ribonucleic acid (miRNA) miR-206 targets the human estrogen receptor-alpha (ERalpha) and represses ERalpha messenger RNA and protein expression in breast cancer cell lines. Mol Endocrinol 2007; 21: 1132-1147.
14) Kondo N, Toyama T, Sugiura H, Fujii Y, Yamashita H. miR-206 Expression is down-regulated in estrogen receptor alpha-positive human breast cancer. Cancer Res 2008; 68: 5004-5008.
15) Dai P, Nakagami T, Tanaka H, Hitomi T, Takamatsu T. Cx43 mediates TGF-beta signaling through competitive Smads binding to microtubules. Mol Biol Cell 2007, 18: 2264-2273.
16) Chang XZ, Li DQ, Hou YF, Wu J, Lu JS, Di GH, Jin W, Ou ZL, Shen ZZ, Shao ZM. Identification of the functional role of peroxiredoxin 6 in the progression of breast cancer. Breast Cancer Res 2007; 9: R76.
17) Zhuang ZG, Di GH, Shen ZZ, Ding J, Shao ZM. Enhanced expression of LKB1 in breast cancer cells attenuates angiogenesis, invasion, and metastatic potential. Mol Cancer Res 2006; 4: 843-849.
18) el-Fouly MH, Trosko JE, Chang CC. Scrape-loading and dye transfer. A rapid and simple technique to study gap junctional intercellular communication. Exp Cell Res 1987; 168: 422-430.
19) Yan LX, Wu QN, Zhang Y, Li YY, Liao DZ, Hou JH, Fu J, Zeng MS, Yun JP, Wu QL, Zeng YX, Shao Y. Knockdown of miR-21 in human breast cancer cell lines inhibits proliferation, *in vitro* migration and *in vivo* tumor growth. Breast Cancer Res 2011; 13: R2.
20) Goldhirsch A, Wood WC, Coates AS, Gelber RD, Thurlimann B, Senn HJ. Strategies for subtypes--dealing with the diversity of breast cancer: highlights of the St. Gallen International Expert Consensus on the Primary Therapy of Early Breast Cancer 2011. Ann Oncol 2011; 22: 1736-1747.
21) Yang L, Wu X, Wang Y, Zhang K, Wu J, Yuan YC, Deng X, Chen L, Kim CC, Lau S, Somio G, Yen Y. FZD7 has a critical role in cell proliferation in triple negative breast cancer. Oncogene 2011; 30: 4437-4446.
22) Stratford AL, Reipas K, Hu K, Fotovati A, Brough R, Frankum J, Takhar M, Watson P, Ashworth A, Lord CJ, Lasham A, Print CG, Dunn SE. Targeting p90 ribosomal S6 kinase eliminates tumor-initiating cells by inactivating Y-box binding protein-1 in triple-negative breast cancers. Stem Cells 2012; 30:1338-1348.

23) Chen X, Xu Z, Wang Y. Recent advances in breast cancer metastasis suppressor 1. Int J Biol Markers 2011; 26: 1-8.

24) Greco SJ, Rameshwar P. MicroRNAs regulate synthesis of the neurotransmitter substance P in human mesenchymal stem cell-derived neuronal cells. Proc Natl Acad Sci USA 2007; 104: 15484-15489.

25) Liu X, He M, Hou Y, Liang B, Zhao L, Ma S, Yu Y. Expression profiles of microRNAs and their target genes in papillary thyroid carcinoma. Oncology Rep 2013; 29: 1215-1220.

26) Song G, Zhang Y, Wang L. MicroRNA-206 targets notch3, activates apoptosis, and inhibits tumor cell migration and focus formation. J Biol Chem 2009; 284: 31921-31927.

27) Adams BD, Cowee DM, White BA. The role of miR-206 in the epidermal growth factor (EGF) induced repression of estrogen receptor-alpha (ERalpha) signaling and a luminal phenotype in MCF-7 breast cancer cells. Mol Endocrinol 2009; 23: 1215-1230.

28) Mese G, Richard G, White TW. Gap junctions: basic structure and function. J Invest Dermatol 2007; 127: 2516-2524.

29) Laird DW. The gap junction proteome and its relationship to disease. Trends Cell Biol 2010; 20: 92-101.

30) Naus CC, Laird DW. Implications and challenges of connexin connections to cancer. Nat Rev Cancer 2010; 10: 435-441.

31) Czyz J. The stage-specific function of gap junctions during tumourigenesis. Cell Mol Biol Lett 2008; 13: 92-102.